SENSING HAND TREMOR IN A VITREORETINAL MICROSURGICAL INSTRUMENT

Mario Gomez-Blanco, Cameron N. Riviere, Pradeep K. Khosla

CMU-RI-TR-99-39

The Robotics Institute
Carnegie Mellon University
Pittsburgh, Pennsylvania 15213

Abstract

An instrument for intraoperative sensing of surgeons' hand tremor during vitreoretinal microsurgery has been developed. Real-time monitoring of tremor is useful to surgeons for purposes of training, adjustment of technique, monitoring of fatigue, and deciding when or whether to perform certain procedures. The instrument incorporates six inertial sensors (three accelerometers and three rate gyros), mounted at the back end of the handle, to detect translation and rotation in six degrees of freedom. The accelerometer data are integrated to obtain translational velocity, and the gyro data are integrated to determine the time-varying rotation matrix needed to transform the instrument motion to a fixed frame of reference. Instrument tip velocity in three dimensions is computed using this information. The displacement amplitude of the tremor is then approximated analytically from the velocity data, approximating it as a sinusoid. Four preliminary tests are presented: 1-dof translation (no rotation); 1-dof translation with amplitude modulation; 3-dof translation (no rotation); 6-dof motion (translation and rotation). The instrument presently estimates oscillations at physiological tremor frequencies with less than 7% error.

Funding is provided by the Johnson & Johnson Focused Giving Program. The authors are grateful to Mr. Peter Berkelman and Dr. Ralph Hollis for the use of the Magnetic Levitation Haptic Interface.

1. Introduction

Positioning error is inherent in normal human hand motion, and limits precision in manual microsurgery [1]. Vitreoretinal microsurgery is a demanding specialty that often involves the need to remove membranes as thin as 20 μm from the front and back of the retina [2]. Physiological tremor is an important source of positioning error [3]. As measured in simulated vitreoretinal microsurgical conditions, tremor at the instrument tip can be as large as 50 μm peak to peak (p-p) [4]. Concern about the inaccuracy it causes has led many microsurgeons to take measures to suppress tremor during surgery, including taking beta blockers, governing consumption of caffeine and alcohol, and making sure to be rested [5, 6]. Presently, the combination of measures taken is largely a matter of personal preference. Research devices such as MADSAM [7] can provide objective measurement of tremor in the laboratory, but once in the operating room, the surgeon's estimate of his own hand tremor continues to be largely subjective. Quantitative intraoperative monitoring of tremor for vitreoretinal as well as other types of microsurgery would be useful for surgical training, and would assist surgeons in making ergonomic adjustments in technique for better results, and in monitoring the effects of fatigue. Surgeons would be able to make informed decisions about when or whether to attempt certain delicate procedures, based on knowledge of their own current tremor amplitude. Intraoperative tremor monitoring would also be of considerable scientific benefit. Presently all studies of tremor in microsurgery rely on data acquired in the laboratory, using microsurgical testbed or simulator setups with varying degrees of authenticity [7]. The ability to monitor tremor during actual delicate microsurgical procedures would of course represent the ultimate in realism in tremor studies, with concomitant increased confidence in the results. Recent years have seen several research efforts in teleoperated ophthalmological microsurgery [8, 9], but manual microsurgery will likely continue to be performed for the foreseeable future, including delicate procedures, and the ability to monitor tremor levels intraoperatively will continue to be beneficial.

To avoid obtruding upon the surgical field or speeding the onset of fatigue in the surgeon, in developing instrumentation for microsurgical tremor monitoring, it is desirable to avoid increasing the weight and size of the instrument. The need to maintain either one or more lines of sight to the instrument, or a mechanical connection to a fixed base, would also be drawbacks. Approaching all these goals simultaneously is problematic. Optical sensing would avoid contact, and likely minimize the added weight, but would require a line of sight. Magnetic sensing would require somewhat more added weight, and would be unlikely to afford the requisite accuracy or resolution for the application, particularly given the ferrous metals used in various surgical hardware. Inertial sensing offers another possibility. It obviates both lines of sight and mechanical connections, and offers both high resolution and high accuracy, particularly in this application, where absolute positioning is not required. Inertial sensors have been made small and are rapidly getting still smaller due to the use of MEMS technology [10]. Currently the size and weight of a six-degree-of-freedom (6-dof) inertial sensor suite that is practical (i.e., uses commercially available parts) are still somewhat larger than would be desired, but the module can be made small and lightweight enough not to obtrude upon the operation. Practical 6-dof inertial sensing in a 1 cm^3 module is likely in the not-too-distant future.

This paper reports on an instrument for intraoperative tremor monitoring in vitreoretinal microsurgery that has been constructed by adding a 6-dof inertial sensor suite to a commercially available instrument, the DP9603 Madlab Pic-Manipulator (Storz Ophthalmics, Inc., St. Louis, Mo.). The Pic-Manipulator was chosen because it is used for extremely delicate manipulation of the retina. The sensor suite is 2.8 cm x 3.3 cm x 4.1 cm and adds approximately 38 g to the instrument, whose original mass is 11 g. Results are presented from preliminary quantitative experiments with oscillations induced by a robotic minimanipulator in the place of the surgeon's hand.

Figure 1. The tremor -monitoring instrument for vitreoretinal microsurgery.

2. Methods

The instrument uses three accelerometers and three angular rate sensors (gyros) for sensing of tremor. Accelerometry is provided by a CXL02LF3 tri-axial low-noise accelerometer (Crossbow Technology, Inc., San Jose, Ca.), and angular rate sensing by three CG-16D ceramic gyros (Tokin Corp., Tokyo). The signals from this sensors are then filtered by a second-order bandpass filter with a low cutoff frequency at 2.5 Hz and a high cutoff frequency at 50 Hz, which reduces noise and provides an anti-aliasing function.

Data are sampled at 1000 Hz using an ADAC 5803HR data acquisition board. The sampled data are again bandpass filtered by a tenth-order Butterworth filter with cutoffs at 7 Hz and 13 Hz, limiting, it is digitally filtered with a band pass filter with low cutoff frequency at 7Hz and with high cutoff frequency at 13 Hz. This limits the signal to precisely the band of interest for physiological tremor [11].

The instrument may be viewed as a rigid body, with the sensors at one end, and the point of interest (the tip) at the other. In the surgeon's hand, the instrument undergoes general, i.e., 6-dof, motion. Let there be a fixed frame, {A}. Consider the motion of a point Q, located on a rigid body to which is affixed a frame, {B}.

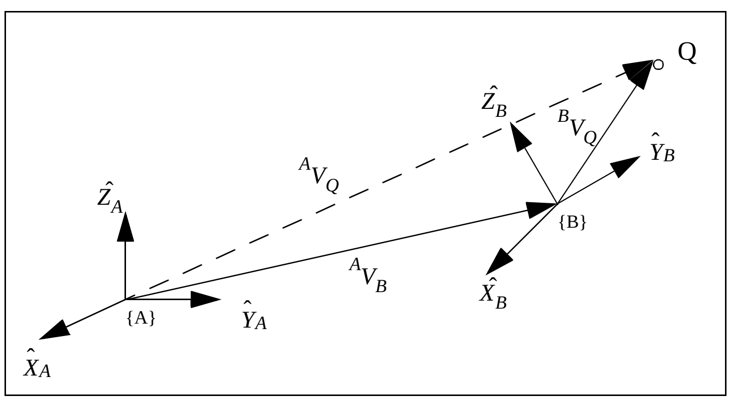

Figure 2. Frame {B} translating and rotating relative to Frame {A}.

Figure 2 depicts the motion of Q relative to both {B} and {A}. The velocity of the instrument tip in {A} is the vector sum of its velocity in {B} and the velocity of {B} in {A}. In this case, since {B} rotates with the rigid body, the velocity of Q in {B} will always be zero. For general motion, the relationship therefore is as follows:

$$ {}^{A}\boldsymbol{V}_{Q} = {}^{A}_{B}\boldsymbol{R}\,{}^{B}\boldsymbol{V} + {}^{A}\Omega_{B} \times {}^{A}_{B}\boldsymbol{R}\,{}^{B}Q \tag{1} $$

where ${}^{B}V$ is the translational velocity of {B} with respect to a frame collocated with {A} but parallel to {B}; this vector is obtained straightforwardly by numerical integration of the accelerometer data. The term ${}^{A}\Omega_{B}$ is the rotational velocity of {B} relative to {A}; this is taken directly from the gyros. The constant vector ${}^{B}Q$ is the fixed position of Q in {B}, determined by the position of the tip with respect to the center of the accelerometer module. The matrix ${}^{A}_{B}R$ represents the current orientation of {B} with respect to {A}, which varies with time.

For tracking the rotation of {B}, an Euler angle formulation [12] is necessary because the sensors rotate with the instrument. A *Z-Y-X* Euler angle formulation is used. Such a formulation treats the rotations represented by each of the three gyros as occurring sequentially, whereas in fact they occur simultaneously. Tracking orientation in general motion can be problematic, since generally multiplication of matrices is not commutative, and therefore different rotational orders result in different results. When the angles involved are very small, however, rotational matrices commute, and adequate results can be obtained for general rotation from a Euler angle formula. This is the benefit of the 1000 Hz sampling: the rotation matrices commute, and the Euler angle order is not critical.

The total rotation occurring in each 1 ms time step can then be represented as:

$$ {}^{A}_{B}\boldsymbol{R}_{Z'Y'X'} = \boldsymbol{R}_{Z}(\alpha)\boldsymbol{R}_{Y}(\beta)\boldsymbol{R}_{X}(\gamma) \tag{2} $$

where the three matrices on the right side of the equation represent the three component rotations of the Z-Y-X Euler formulation. The resulting matrix is

$$ {}^{A}_{B}\boldsymbol{R}_{Z'Y'X'} = \begin{bmatrix} \cos(\alpha)\cos(\beta) & \cos(\alpha)\sin(\beta)\sin(\gamma) - \sin(\alpha)\cos(\gamma) & \cos(\alpha)\sin(\beta)\cos(\gamma) + \sin(\alpha)\sin(\gamma) \\ \sin(\alpha)\cos(\beta) & \sin(\alpha)\sin(\beta)\sin(\gamma) + \cos(\alpha)\cos(\gamma) & \sin(\alpha)\sin(\beta)\cos(\gamma) - \cos(\alpha)\sin(\gamma) \\ -\sin(\beta) & \cos(\beta)\sin(\gamma) & \cos(\beta)\cos(\gamma) \end{bmatrix} \tag{3} $$

The rotations are cumulative; at each time step the existing rotation matrix must be premultiplied by the new rotation matrix to keep track of the orientation. At time k=0, the rotation matrix ${}^{A}_{B}R$ is equal to the identity matrix, and at each subsequent time step k,

$$ {}^{A}_{B}\boldsymbol{R}_{k} = \left({}^{A}_{B}\boldsymbol{R}_{Z'Y'X'}\right)_{k}\,{}^{A}_{B}\boldsymbol{R}_{k-1} \ . \tag{4} $$

Using this, (1) then yields the instrument tip velocity. It is possible to obtain tip position from velocity by another numerical integration. However, inertial sensor noise and drift tend to be accumulated by integration, corrupting the signal. It was impossible to avoid the first integration, but would be desirable to avoid a second one. Since tremor is defined as roughly sinusoidal [11], the tip position, ${}^{A}P_{Q}$, can be approximated analytically from the velocity as follows:

$$ {}^{A}\boldsymbol{P}_{Q} = \frac{1}{2\pi f}\,{}^{A}\boldsymbol{V}_{Q} \tag{5} $$

where f is the frequency of the oscillation. Numerous techniques to estimate f could be used; presently f is estimated by determining the length of the ten most recent cycles of the velocity (determined by the 20 most recent zero-crossings).

Initial testing of the instrument was conducted using the Magnetic Levitation Haptic Interface of Berkelman *et al*. [13] in place of the surgeon's hand. The MLHI is a 6-dof high-bandwidth, high-precision manipulator. Four preliminary tests were conducted:

- 1-dof translation;
- 1-dof translation with amplitude modulation;
- 3-dof translation;
- 6-dof motion.

All oscillations were at approximately 11 Hz. Translations were roughly 30 μm p-p and rotations roughly 9° p-p. The amplitude-modulated translation varied from 30 μm to 80 μm p-p at 1 Hz. Test durations varied from 1 to 5 seconds.

Table 1: Results from unmodulated tests

Type of motion	Tip motion coord.	rms error of tip displmt. (mm)	rms expected signal (mm)	rms sensed signal (mm)	ratio (sensed/ expected)
1-dof translation	*Z*	0.0033	0.0106	0.0113	1.0660
3-dof translation	*X*	0.0032	0.0096	0.0097	1.0104
3-dof translation	*Y*	0.0031	0.0097	0.0100	1.0300
3-dof translation	*Z*	0.0027	0.0108	0.0112	1.03700
6-dof motion	*X*	0.1414	0.7239	0.6874	0.9495
6-dof motion	*Y*	0.1701	0.8323	0.7840	0.9419
6-dof motion	*Z*	0.0076	0.0367	0.0349	0.9509

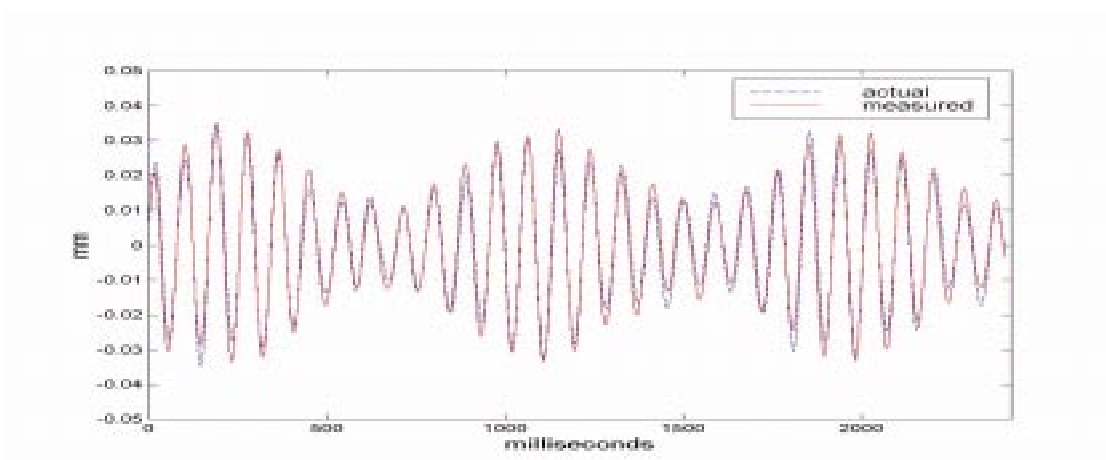

Figure 3. System operation on 1-dof translation at 11 Hz, with amplitude modulation at 1 Hz from 30 mm to 80 mm p-p. The black dashed line shows the motion as sensed by the manipulator generating it, and the solid gray line the motion as sensed by the surgical instrument.

3. Results

For each unmodulated trial, the first column of data in Table 1 presents the root-mean-square (rms) error of the tip displacement obtained from (5) with respect to the sensor data from the MLHI manipulator itself. For the same set of trials, the remaining columns of Table 1 show the overall rms amplitude of the motion in each test, and the ratio of rms amplitude sensed by the instrument to rms amplitude sensed by the manipulator.

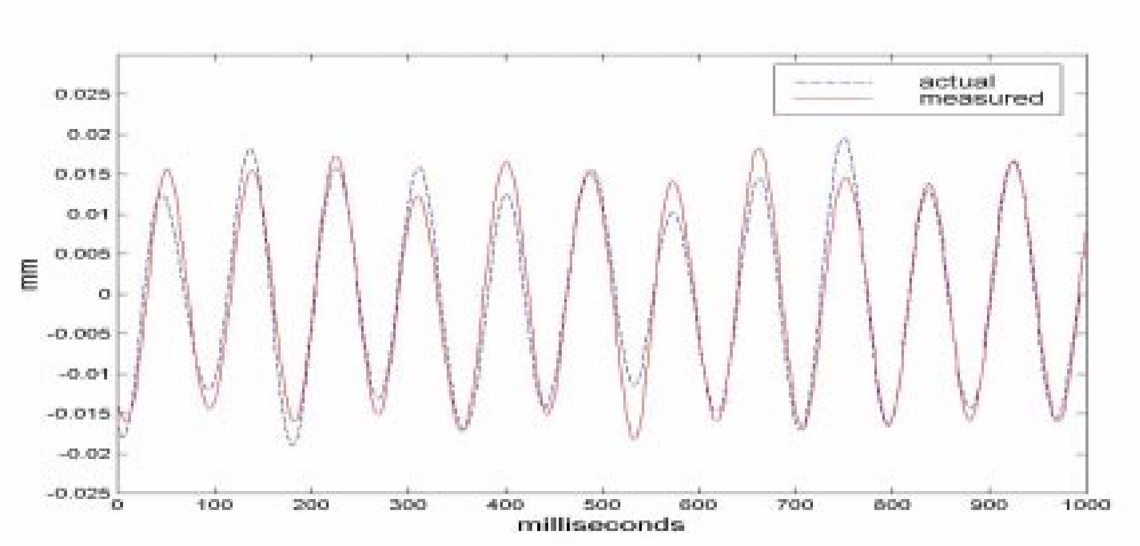

(a)

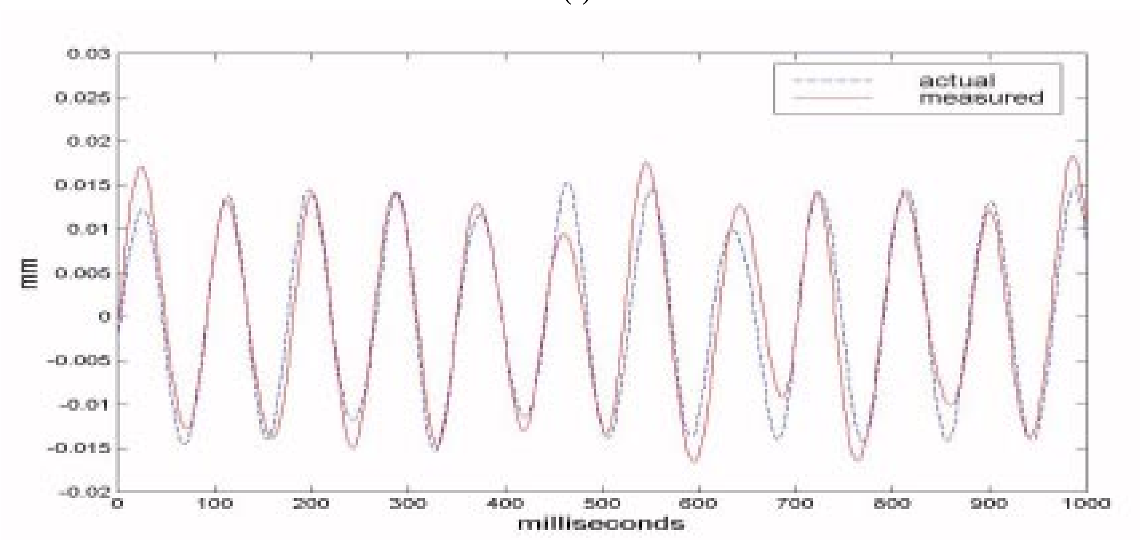

(b)

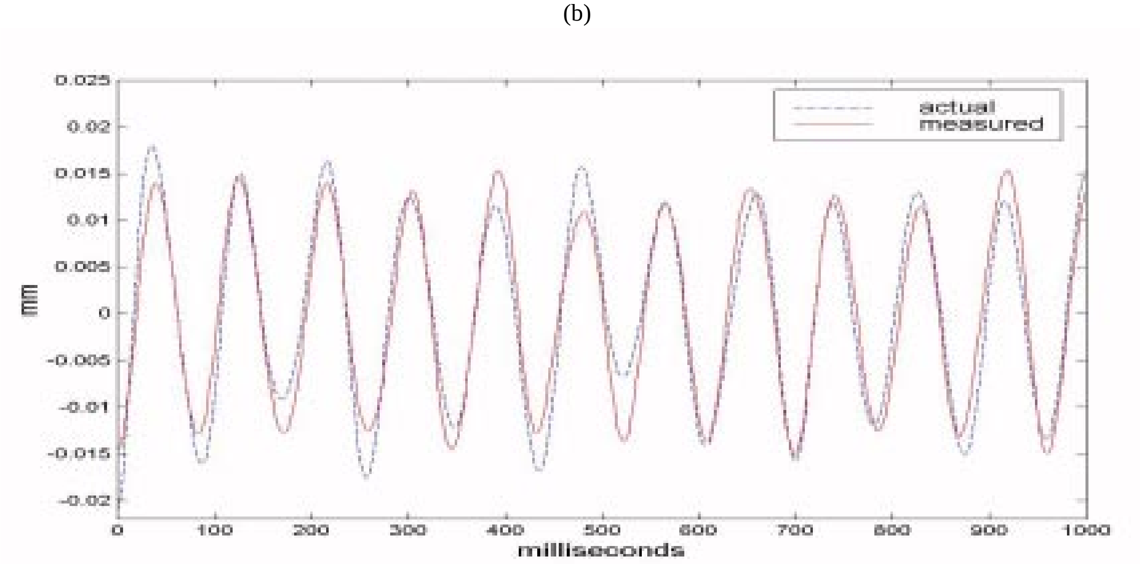

(c)

Figure 4. Results from triaxial translation with no rotation. The dashed line shows the motion as sensed by the manipulator generating it, and the gray line the motion as sensed by the instrument. (a) Z. (b) Y. (c) X.

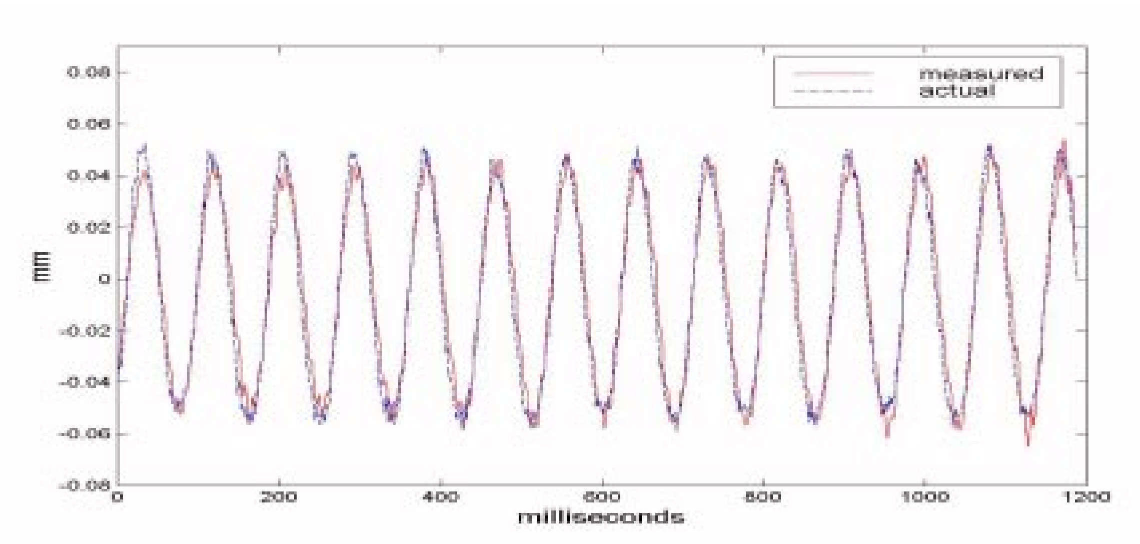

(a)

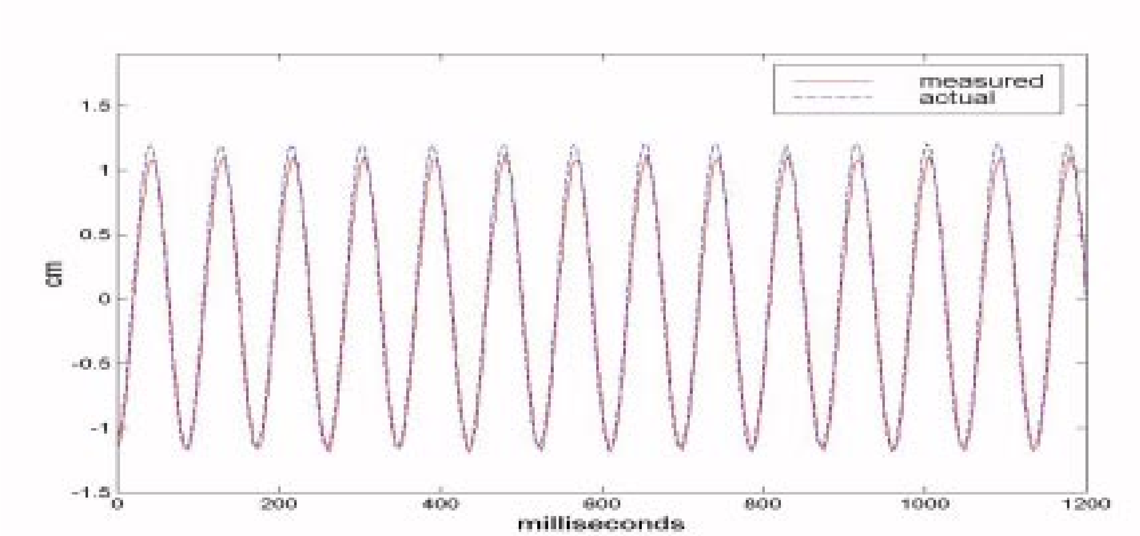

(b)

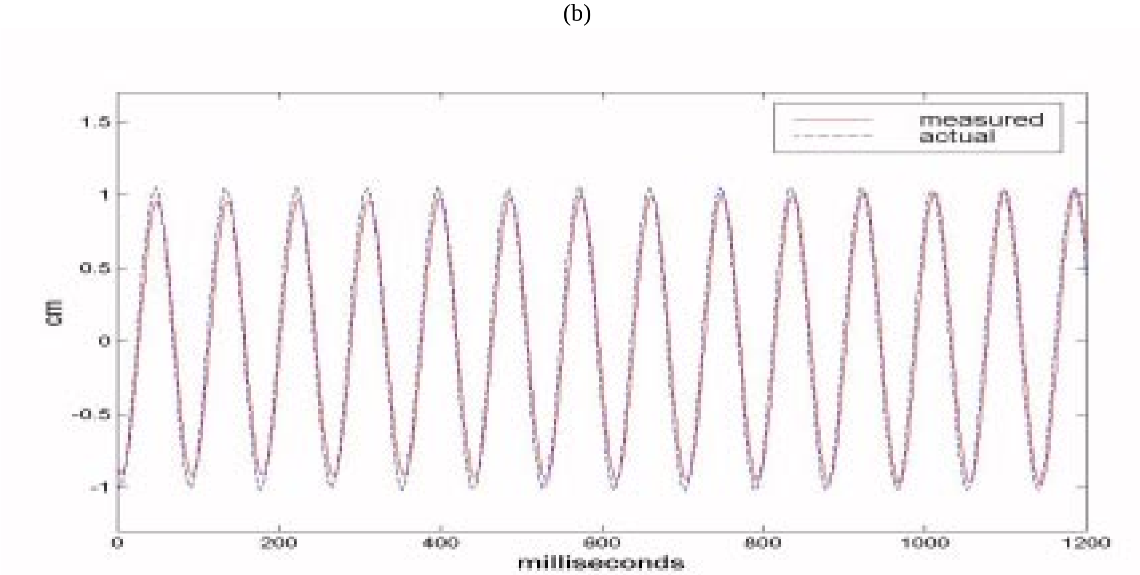

(c)

Figure 5. Results from 6-dof motion. The dashed line shows the motion as sensed by the manipulator generating it, and the gray line the motion as sensed by the instrument. (a) Z. (b) Y. (c) X.

Figures 3, 4 and 5 present samples of results. Figure 3 presents the results of the amplitude modulated test. Figure 4 shows results from the 3-dof translation test for the (*x*,*y*,*z*) motion of the tip. Figure 5 displays results from the 6-dof motion test, in which the (*x*,*y*,*z*) motion of the instrument tip is affected not only by the translations but also the rotations generated by the manipulator. The filtering utilized in the instrument causes phase lag in the results, which is not depicted here. The instrument data have been time-shifted in the figures to show the correspondence between input and output cycles of the oscillation. Figure 6 presents a sample of tremor recorded from a human subject using the instrument.

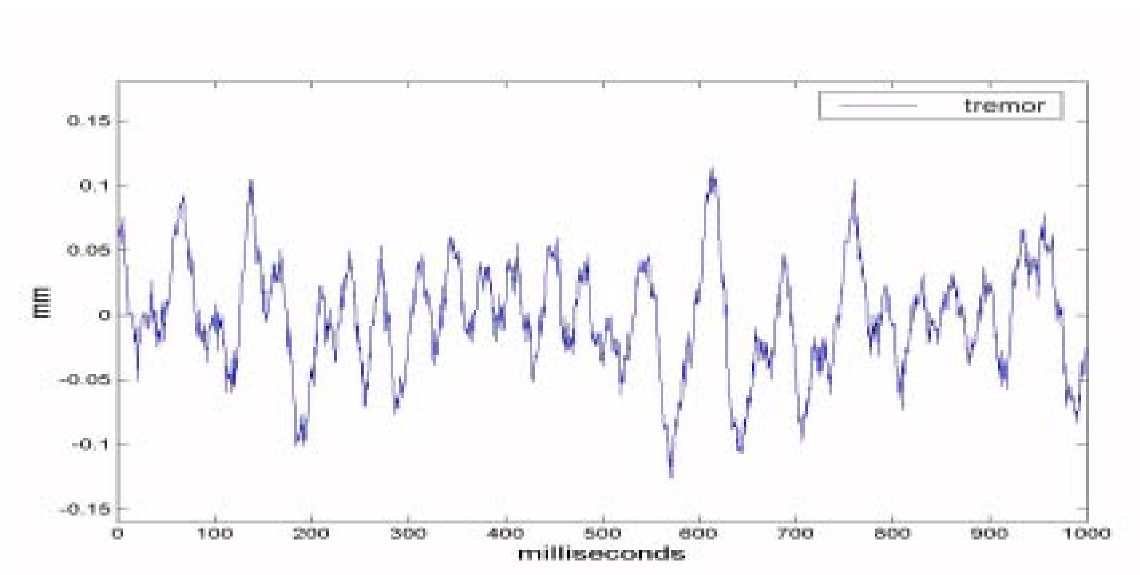

Figure 6. Sample of actual hand tremor using the instrument (one coordinate of data presented).

4. Discussion

The results from these tests demonstrate the ability of the tremor monitoring instrument to accurately measure oscillations in the nominal frequency band of physiological tremor. Full time histories of measured data are presented here, in order to demonstrate the performance of the system. However, during actual surgery, this is more information than the surgeon needs or can likely use. The aim of the system for actual intraoperative use is therefore to report to the surgeon an estimate of the peak-to-peak tremor, updated at a user-friendly rate, perhaps 0.5 Hz. As the matter of primary interest to the surgeon is the effective width of the tremor envelope, the appropriate quantity to report is the maximum peak-to-peak amplitude detected during a given display update interval. One of our vitreoretinal microsurgical colleagues has expressed a desire to have auditory rather than visual presentation of this information, and this will therefore be implemented.

Testing of the instrument proceeds next to recorded human motion and then to actual human subject evaluations. This work will require modification of the system to compensate for the effect of gravity on the data. The gravity vector with respect to the instrument varies with time as the instrument is rotated. Variations due to slow rotations will be suppressed by the bandpass filtering; however, rapid rotations could produce signal content in or near the tremor band, which would then be mistaken as part of the tremor signal if not compensated for. Work is underway to implement gravity compensation using the existing sensors.

Additional ongoing research involves further reduction in noise and other errors that accumulate during integration. Continuing improvement in sensing accuracy will allow the use of greater bandwidth, enabling measurement not only of tremor but of a wide band of involuntary and voluntary motion, again both for intraoperative clinical use and for scientific purposes. This instrument also represents a fundamental step in the development of active tremor compensation in a hand-held instrument [14].

5. Conclusion

An instrument for real-time intraoperative monitoring of surgeons' hand tremor during vitreoretinal microsurgery has been developed by fitting a commercial instrument used for delicate retinal procedures with a suite of three MEMS-based accelerometers and three rate gyros. The system has been tested in 1-, 3-, and 6-dof motion with stationary and amplitude modulated sinusoidal oscillations.

References

[1] Patkin, M.: Ergonomics applied to the practice of microsurgery. Austr. N. Z. J. Surg. **47** (1977) 320-239

[2] Charles, S.: Dexterity enhancement for surgery. In: Taylor, R. H., Lavallée, S., Burdea, G. C., Mösges, R. (eds.): Computer Integrated Surgery: Technology and Clinical Applications. MIT Press, Cambridge (1996) 467-471

[3] Harwell, R. C., Ferguson, R. L.: Physiologic tremor and microsurgery. Microsurgery **4** (1983) 187-192

[4] Riviere, C. N., Rader, R. S., Khosla, P. K.: Characteristics of hand motion of eye surgeons. Proc. 19th Annu. Conf. IEEE Eng. Med. Biol. Soc., Chicago (1997)

[5] Humayun, M. U., Rader, R. S., Pieramici, D. J., Awh, C. C, de Juan, E., Jr.: Quantitative measurement of the effects of caffeine and propranolol on surgeon hand tremor. Archives of Ophthalmology **115** (1997) 371

[6] Lakie, M., Frymann, K., Villagra, F., Jakeman, P.: The effect of alcohol on physiological tremor. Experimental Physiology **79** (1994) 273-276

[7] Rader, R. S., Walsh, A. C., Awh, C. C., de Juan, E., Jr.: Manual stability analysis of vitreoretinal microsurgery tasks. Ergonomics, in review

[8] Hunter, I. W., Doukoglou, T. D., Lafontaine, S. R., Charette, P. G., Jones, L. A., Sagar, M. A., Mallinson, G. D., Hunter, P. J.: A teleoperated microsurgical robot and associated virtual environment for eye surgery. Presence **2** (1993) 265-280

[9] Schenker, P. S., Barlow, E. C., Boswell, C. D., Das, H., Lee, S., Ohm, T. R., Paljug, E. D., Rodriguez, G., Charles, S. T.: Development of a telemanipulator for dexterity enhanced microsurgery. Proc. 2nd Intl. Symp. Med. Robot. Comput. Assist. Surg. Wiley, New York (1995) 81-88

[10] Weinberg, M., Bernstein, J., Borenstein, J., Campbell, J., Cousens, J., Cunningham, B., Fields, R., Greiff, P., Hugh, B., Niles, L., Sohn, J.: Micromachining inertial instruments. In: Micromachining and Microfabrication Process Technology II. Proc. SPIE, vol. 2879 (1996) 26-36

[11] Elble, R.J., Koller, W.C.: Tremor. Johns Hopkins University Press, Baltimore (1990)

[12] Craig, J.: Robotics: mechanics and control. Addison-Wesley (1989) 19-59

[13] Berkelman, P. J., Butler, Z. J., Hollis, R. L.: Design of a hemispherical magnetic levitation haptic interface device. Proc. ASME IMECE, Atlanta, DSC Vol. 58 (1996) 483-488

[14] Riviere, C. N., Rader, R. S., Thakor, N. V.: Adaptive canceling of physiological tremor for improved precision in microsurgery. IEEE Trans. Biomed. Eng. **45** (1998) 839-846